Long-Term Field Monitoring of Lateral Loads in Semi-Integral Bridge Foundations

Behdad Mofarraj[1] and Jorge G. Zornberg, Ph.D., P.E., F.ASCE[2]

[1]Ph.D. Candidate, Dept. of Civil, Architectural, and Environmental Engineering, Univ. of Texas at Austin, Austin, TX. Email: mofarraj@utexas.edu
[2]Dept. of Civil, Architectural, and Environmental Engineering, Univ. of Texas at Austin, Austin, TX. Email: zornberg@mail.utexas.edu

ABSTRACT

Jointless bridge designs have become increasingly common over the past several decades, both in the USA and worldwide. The increasing adoption of this alternative is largely due to the poor long-term performance of expansion joints and often prohibitive cost of joint maintenance. While integral bridges typically require flexible foundations to accommodate deck thermal movements, most transportation agencies do not require flexible foundations for semi-integral bridges. This is because, unlike integral bridges, the superstructure of a semi-integral bridge is not directly connected to the abutment and therefore is not expected to experience lateral loading. In this study, 1.5 years of data collected from the drilled shaft foundations of a semi-integral bridge in Texas is presented. This data indicates that semi-integral bridge foundations can also experience significant cyclic lateral loading. In this case, the largest bending moments were observed during the colder months of the year, when the superstructure experiences maximum shrinkage due to temperature decrease.

INTRODUCTION

Semi-integral and integral bridge construction is becoming increasingly common, both in the USA and worldwide. The main characteristic of these bridges is the elimination of expansion joints at the ends of the deck and in between spans. However, the abutment wall and abutment caps are not integrally connected to allow the superstructure to move independently from the substructure. Unlike semi-integral bridges, integral bridges are continuous single- or multi-span bridges in which the superstructure is constructed integrally with the substructure.

The increasing popularity of these structures can be attributed to the number of issues associated with deck expansion joints. Deck expansion joints are typically used to alleviate stresses in the structure caused by phenomena associated to shrinkage, creep, thermal expansion/contraction, and differential settlement of piers and abutments (Burke, 2009). However, as noted in Purvis and Berger (1983), several problems are associated with deck expansion joints, including the high rate of wear and tear, exposure of the structure to harmful chemicals and relatively high cost of initial construction and maintenance. Therefore, many transportation agencies throughout the world have opted for other alternatives such as semi-integral and integral bridges.

A brief look at the semi-integral and integral bridge details from within the United States alone reveals significant differences among the designs adopted in each state. For example, according to Maruri and Petro (2005), while many states require H-pile foundations oriented towards the weak bending axis for integral bridges to increase flexibility, some states require them to be oriented towards the strong axis and some even allow the use of drilled shafts which are typically more rigid than H-piles. Moreover, while lateral loading is considered in the design

of integral bridge foundations, such loading has typically not been considered in the design of semi-integral bridge foundations. These discrepancies are further reflected in the development of instrumentation programs implemented to monitor the behavior of integral and semi-integral bridges. While long-term studies on the behavior of integral abutment foundations could be identified (Ooi et al, 2010; Lawver et al, 2000; Abendroth et al, 2005), the authors were not able to find studies on lateral loading of semi-integral bridge foundations in the technical literature.

Despite the lack of focus on possible lateral loading of semi-integral bridge foundations, a prior investigation of the behavior of a pilot semi-integral bridge in Texas, described in Mofarraj and Zornberg (2022), found evidence of lateral movements in the abutment caps though the magnitude of the loads remained unknown. Applying the lessons learned from the pilot instrumentation program, a more comprehensive bridge monitoring program was developed for a second semi-integral bridge in Texas which involved over 70 sensors and included a dedicated foundation monitoring system.

The purpose of this study is to provide an analysis of the data obtained from monitoring lateral deformations of the foundation elements in the semi-integral China Creek Bridge and characterize the deflection and lateral loads acting on the bridge foundations due to thermal expansion and contraction of the superstructure.

DESCRIPTION OF CHINA CREEK BRIDGE

The semi-integral China Creek Bridge is a state highway bridge built in 2020, outside of Wichita Falls, TX. A schematic of this bridge is shown in Figure 1. The bridge is 27.5 m long and has two traffic lanes. The superstructure includes prestressed concrete I-beam girders, precast concrete panels between the girders, and a cast-in-place reinforced concrete overlay. The abutment walls are integrally connected to the deck and are 1.25 m deep. The bridge is supported by four 11 m deep drilled shafts on each side, which are 0.9 m in diameter each. The deck connects to the approaching roadway via 6-m long reinforced concrete approach slabs that are structurally connected to the deck and abutment wall on one end and rest on sleeper slabs on the other. The gap between the abutment wall and abutment cap was filled with a 50 mm thick closed cell foam as displayed in Figure 1.

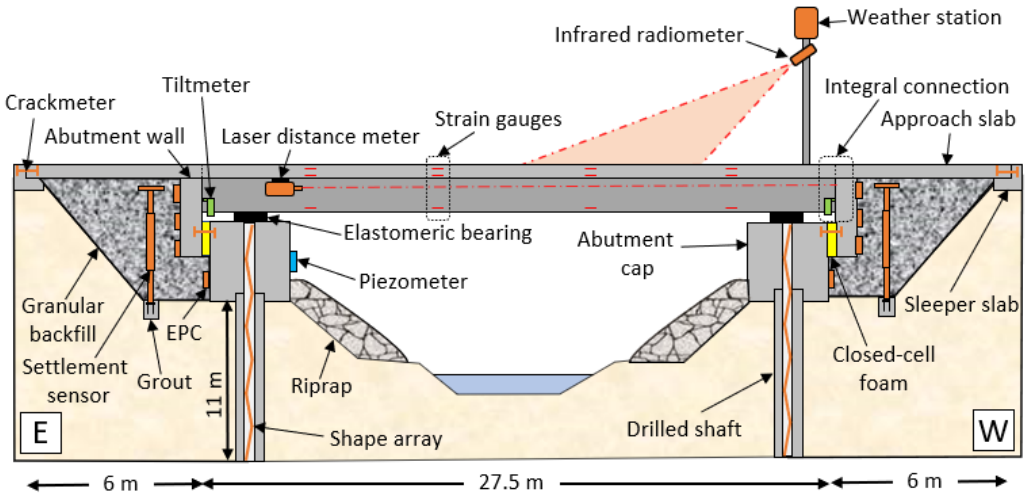

Figure 1. Schematic of the semi-integral China Creek Bridge and the installed sensors (Note: EPC: Earth Pressure Cell)

While forming the abutment walls, a very stiff closed cell foam was used on the inner facing of the abutment walls. Although most of this material was removed after the construction, the portion between the abutment cap and abutment wall was left in place (See Figure 1). Considering the stiffness of this material, it was expected that the contraction of the deck due to shrinkage and changes in temperature would likely contribute to lateral deflection of the drilled shafts. Furthermore, the development of friction and shear at the base of the elastomeric bearing pads due to expansion and contraction of the deck may also induce lateral loads acting on the drilled shafts in spite of the semi-integral nature of the bridge (Han et al., 2019).

GEOTECHNICAL CHARACTERIZATION OF THE FOUNDATION SOIL

Prior to bridge construction, 12 m deep borings were conducted on each side of the bridge for subsurface characterization. The materials recovered from these borings on the top 4 m revealed the presence of lean soft clay deposits. Specifically, the material recovered from 2.2 m to 4 m deep were described as very soft and saturated. Below 4 m, the recovered materials involved mainly stiff and dry lean clay, while the soil below 7 m appeared very hard and blocky.

In addition to the physical characterization of the in-situ soils, a series of Texas Cone Penetration (TCP) (TEX 132-E, 1999) tests were performed at 1.5 m intervals. A TCP count of 50 (maximum blow count) was reached for depths below 4 m, making it a well-suited bearing stratum for drilled shaft foundation. However, the top 4 m of the boring logs consisted of soils with TCP counts ranging from 3 to 7, which is associated with soft to medium soils, according to Touma and Reese (1972). Considering the characteristics of this top soil layer, a decision was made to protect the drilled shafts from side-wall caving using 4 m long steel casings.

INSTRUMENTATION OVERVIEW

During the construction of China Creek Bridge, over 70 sensors were installed to monitor various aspects of the bridge behavior and performance. The installed sensors are shown in Figure 1. This paper focuses on the data collected to monitor the lateral displacements on the drilled shaft elements of this semi-integral bridge.

The lateral displacements of drilled shafts were obtained using shape arrays (Measurand SAAV), which were installed during bridge construction within the drilled shafts. They consist of a series of rigid segments connected with joints that allow movement in any direction but prevent twisting. Each segment is instrumented with a triaxial MEMS (Micro-Electro-Mechanical Systems) gravity sensors for measuring tilt in two perpendicular directions. The sensor data is used to calculate the relative position of each joint compared to other joints. Therefore, by knowing the absolute position of one joint, the position of all other joints can be calculated. In this paper, the bottom of the drilled shaft is assumed stationary under normal operating conditions for calculating the absolute displacement of the abutment caps. The potential errors associated with this assumption will be discussed in the next section. According to the manufacturer, this instrument has a precision of ±0.5 mm for a 30 m array.

Figure 2 shows the installation of the drilled shaft rebar cage (fitted with a 70 mm PVC conduit) as well as the installation of the shape array in one of the drilled shafts of China Creek Bridge. The shape arrays used in this study consist of 22 segments of 0.5 m in length each which provide a 3-D deformation profile of the drilled shafts. While continuous data collection began in October 2020, initial sensor readings were recorded immediately after installation of the shape arrays in June 2020 and before placement of the bridge girders.

(a) (b)

Figure 2. (a) Installation of the drilled shaft rebar cage fitted with a shape array casing (b) installation of shape array inside the casing after the abutment caps were formed

METHODOLOGY FOR DATA ANALYSIS

With the shape arrays installed, the deflection profile of the drilled shafts are calculated by finding the change in position of each node compared to its position at the time of installation. Figure 3(a) shows a schematic view of the instrumented drilled shafts and the surrounding soil layers. Two of the deflection profiles obtained using shape arrays for the west abutment drilled shaft are presented in Figure 3(b). The displayed data correspond to the deflection profile of the drilled shaft on two occasions during the first fall and winter after bridge completion. As the shape array data indicates, the instrumented drilled shaft has bent towards the center of the bridge due to thermal contraction of the superstructure. The shape of the deflection profiles resembles short pile behavior (Broms, 1964) and indicates that the foundation is most likely rotating about a point within the hard clay layer. While determining the position of this point can slightly affect the displacement estimates for all points along the drilled shafts, it will not affect the calculation of curvature and bending moments which is the primary focus of this paper.

After obtaining the deflection profile of a drilled shaft, other important information can be predicted, including the bending moment profile of the drilled shafts. To do so, the curvature profile of the foundation needs to be initially calculated. Mathematically, the curvature profile can be obtained by taking the second derivative of the deflection profile. In this study, the second derivative is approximated using the Finite Difference Method (FDM), as follows:

$$\frac{d^2y}{dx^2} \approx \frac{y_{m+1} - 2y_m + y_{m-1}}{h^2}$$

In this equation, "*y*" is the nodal lateral deflection and "*h*" is the segment length, as displayed in Figure 4. Because the shape array only provides discrete displacement measurements at the nodal locations, calculating the second derivative of the shape array deflection profile using FDM can introduce errors due to the precision limits of the instrument as well as due to truncation errors. Consequently, a Savitzki-Golay filter was applied on the lateral deflection data to smooth the raw data prior to derivation. The calculated curvature profiles are presented in Figure 3(c). Interestingly, in both instances, the maximum curvature appears to occur at a depth of around 4.3 m, right below the drilled shaft casing termination depth and top soft soils transition into comparatively stiffer soil layers.

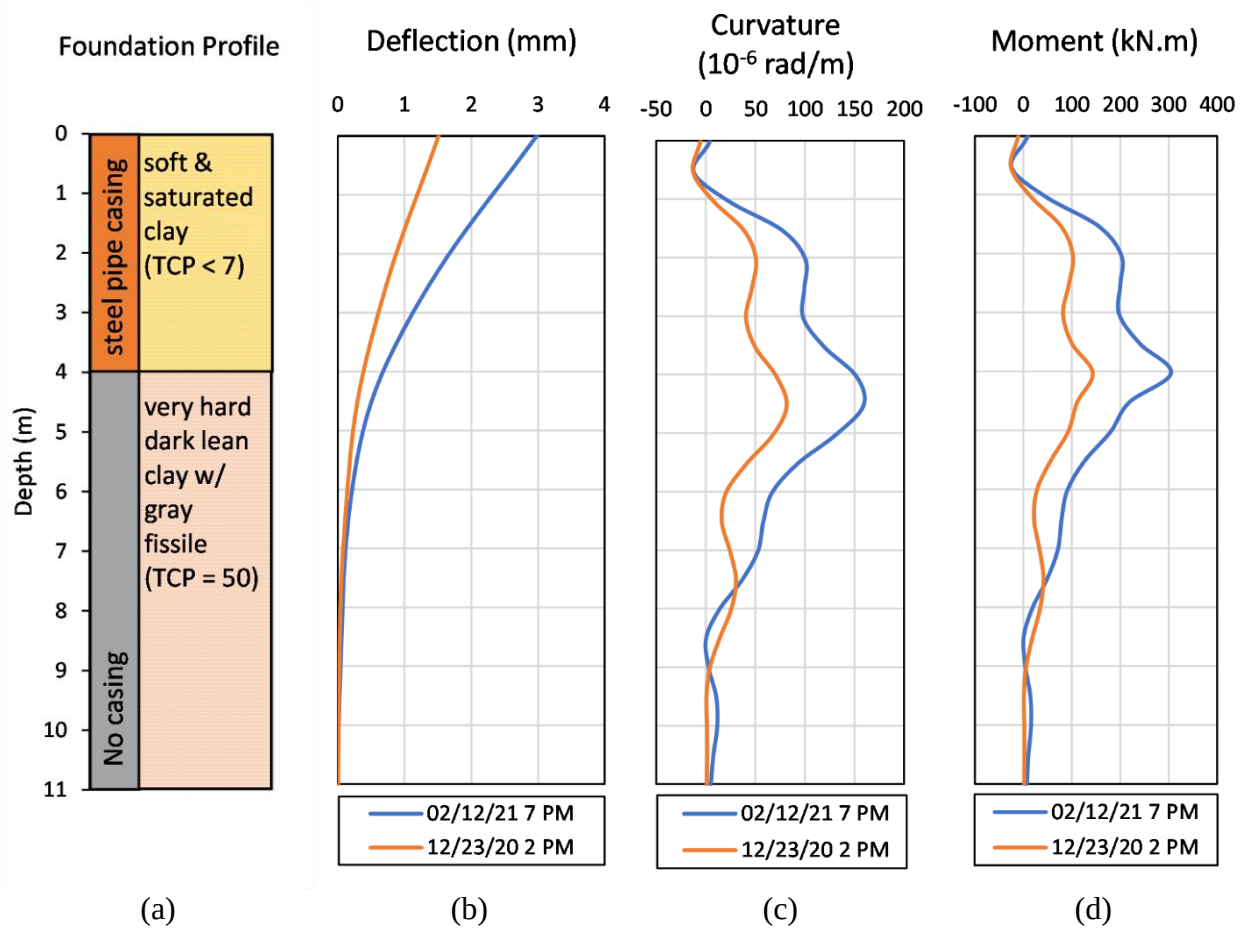

Figure 3. Profiles for the west abutment drilled shaft profiles on two different dates: (a) subsurface profile (b) lateral deflection profile (c) curvature profile, and (d) flexural moment profile

To estimate the flexural moment profile of a drilled shaft, flexural stiffness properties of the instrumented sections were defined using the LPILE software (Wang et al., 2022). This analysis involved calculating separate flexural stiffness properties for both the top portion (encased) and the remaining segments of the drilled shaft. The resulting moment profile is shown in Figure 3(d). In the two instances graphed, maximum bending moments of 150 and 300 kN.m were observed at the depth of 4 m below the ground surface (Bottom of the casing).

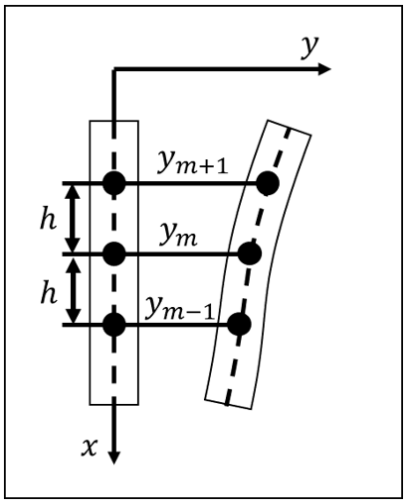

Figure 4. Schematic view of a deflected drilled shaft

It is worth noting that the calculated curvature profile may have been slightly affected by truncation errors which is a known artifact and limitation of FDM for calculating derivatives. The accuracy of these results could be further verified by conducting additional p-y analysis or other numerical methods. However, this additional analysis would be outside the scope of this study. The main focus of this study is to present the collected data that provides proof of cyclic lateral loading of semi-integral bridge foundations which is typically unaccounted for in the design and analysis of semi-integral bridges.

The procedure described above can be used to evaluate the maximum moment acting on the drilled shafts at any point in time, particularly considering the cyclic nature of the temperature-induced lateral movements. In particular, the maximum moment induced by lateral loads acting on the drilled shafts due to thermal expansion/contraction of the superstructure, can be compared with a section's cracking moment. This comparison can provide a measure of the level of elastic flexural capacity that has been reached in a section.

RESULTS AND DISCUSSION

The time history of the lateral displacements measured at the abutment cap, maximum bending moments acting on the drilled shafts, and ambient air temperature are plotted in Figure 5.

The abutment cap displacement records measured by the shape arrays are plotted in Figure 5(a). In this time-history, positive values indicate abutment cap movement toward the center of the bridge. It can be seen that both abutment caps have experienced sub-millimeter magnitude cycles of displacement every day. Moreover, this data indicates that the two abutment caps have not experienced the same level of lateral deformation, with generally larger magnitude displacements recorded for the west abutment cap compared to the east abutment cap.

The observed asymmetry can be attributed to slight differences to the resistance of the abutment and foundation soils against thermal expansion/contraction of the bridge. For example, it was noticed that a lower compaction effort was used during the west abutment backfill placement compared to the east abutment.

Overall, the west abutment cap has moved by 2 mm toward east at the end of the first-year cycle (June 2021) compared to its initial position (June 2020). In contrast, the east abutment cap

appears to have remained within 1 mm of its initial position for the majority of the monitoring period and have returned to its initial position recorded in June 2020 at the end of the first-year cycle (June 2021). In both cases, the largest displacements are observed during the coldest times of the year during which the superstructure experiences maximum thermal contraction. It is worth noting that the large spike observed in February 2021 is due to winter storm Uri, which affected the entire state of Texas as well as many other states across the United States.

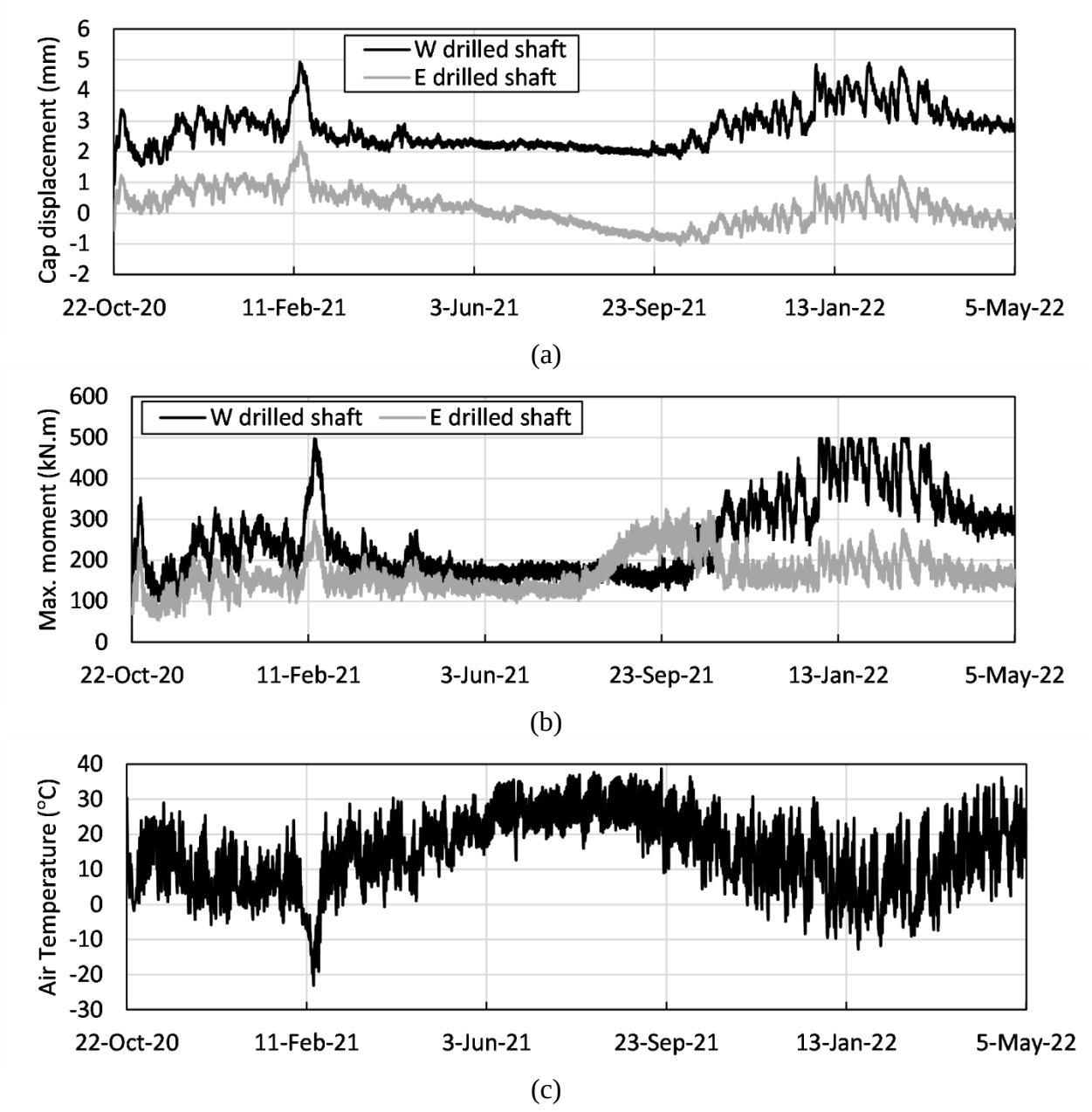

Figure 5. (a) Abutment cap displacement time histories relative to the time of construction (b) maximum moments acting on the drilled shafts (c) Ambient air temperature time history (Drilled shafts' zero readings taken in June 2022)

Seasonally, both abutment caps are observed to experience the smallest displacement cycles during the warm months of the year (April to October), with temperatures not typically changing by more than 15°C in a given time period. In comparison, significantly larger displacement cycles are observed during the late fall and winter (November to April) with temperatures typically changing by up to 30°C within just a few days, as indicated in Figure 5(c).

Considering the bending moment time history data plotted in Figure 5(b), it can be seen that the west abutment drilled shaft has typically experienced larger maximum moments compared to the east abutment. However, a different foundation behavior is observed in the period of July to October 2021. In this period, the east abutment cap has experienced more displacement towards the backfill, while the west abutment cap has remained nearly stationary. Consequently, larger bending moments were observed for the east drilled shaft compared to the west drilled shaft in this period as well.

Consistent with the pattern observed for the abutment cap deflection data, comparatively larger bending moment cycles were observed during the colder months of the year as well. While the calculated bending moments are within the estimated elastic range of flexural behavior for the drilled shaft sections (smaller than 500 kN.m), the observed behavior reveals that the magnitude of the bending moments is not negligible and may benefit from evaluation of the long-term effects of the loading cycles, including fatigue analysis of the foundation elements to assess the service life of the structure. Several examples of low cycle fatigue analysis are documented in the literature for reinforced concrete piles and integral bridge foundations (Karalar and Dicleli, 2016; Fawaz and Murcia, 2021), which can be relevant to semi-integral bridges as well.

Overall, the drilled shafts in the semi-integral China Creek Bridge were clearly observed to experience cyclic lateral loading due to thermal expansion/contraction of the superstructure. This load is not necessarily evenly distributed between the abutments and can reach values as high as the section's cracking moment. To improve the long-term performance of these structures, it is suggested that the design engineers recognize the possibility of these loads, modify abutment details to minimize this interaction and design for this type of loading.

CONCLUSIONS

The foundation monitoring data obtained from a pilot semi-integral bridge constructed near Wichita Falls, TX was evaluated to assess the magnitude of lateral loading experienced by the foundation elements due to thermal expansion/contraction of the superstructure. Deflection data was collected from the shape arrays and the collected data was used to calculate the bending moment profile of the instrumented drilled shafts as well as the maximum bending moment acting on them.

The instrumentation data collected from the bridge foundation reveals the following conclusions:

- Despite the lack of an integral connection between the superstructure and foundation elements in this semi-integral bridge, the foundation elements have clearly experienced lateral loads due to thermal expansion/contraction of the superstructure.
- The shape array sensors were able to successfully collect the displacement data needed to define the deflection profile of the drilled shafts in both abutments. The collected data indicates that the abutment caps moved by up to 5 mm toward the center of the bridge due to bridge contraction in the winter.

- In spite of the symmetric geometry of the bridge, the shape array data revealed that the lateral displacements in the drilled shafts were not necessarily symmetrical. Consequently, the west abutment drilled shafts have experienced larger magnitude deflections compared to the east abutment. This asymmetrical behavior may be due to uneven compaction of the abutment backfills, which can lead to uneven abutment backfill stiffnesses against lateral expansion of the bridge superstructure.
- The deflection and bending moment cycles affecting the drilled shafts were found to be significantly larger during the colder months of the year, when larger temperature fluctuations are experienced, as compared to the warmer months of the year.
- The observation of drilled shaft bending moments reaching values close to the section's cracking moment on several occasions indicates that it is crucial to design semi-integral bridge foundations for lateral loading due to thermal expansion/contraction of the bridge.
- The maximum bending moment was typically observed at the depth of 4 m below the ground surface, where the casing is terminated.

ACKNOWLEDGEMENTS

The authors would like to thank Texas Department of Transportation for funding this research under project 0-6936 through the Center for Transportation Research at the University of Texas at Austin.

REFERENCES

Abendroth, R. E., Greimann, L. F., Lim, K.-H., Sayers, B. H., Kirkpatrick, C. L., and Ng, W. C. (2005). *Field Testing of Integral Abutments*. Iowa State University Center for Transportation Research and Education, Ames, IA.

Broms, B. B. (1964). "Lateral Resistance of Piles in Cohesive Soils." *Journal of the Soil Mechanics and Foundations Division*, 90 (2), 27–63.

Burke, M. P. (2009). *Integral and Semi-Integral Bridges*. Wiley-Blackwell.

Fawaz, G., and Murcia-Delso, J. (2021). "Three-Dimensional Finite Element Modeling of RC Columns Subjected to Cyclic Lateral Loading." *Engineering Structures*, 239: 112291.

Han, L., Belivanis, K. V., Helwig, T. A., Tassoulas, J. L., Engelhardt, M. D., and Williamson, E. B. (2019). "Field And Computational Investigation of Elastomeric Bearings in High-Demand Steel Girder Application." *Journal of Constructional Steel Research*, 162: 105758.

Karalar, M., and Dicleli, M. (2016). "Effect of Thermal Induced Flexural Strain Cycles on The Low Cycle Fatigue Performance of Integral Bridge Steel H-Piles." *Engineering Structures*, 124, 388–404.

Lawver, A., French, C., and Shield, C. K. (2000). "Field Performance of Integral Abutment Bridge." *Transportation Research Record*, 1740 (1): 108–117. SAGE Publications Inc.

Maruri, R. F., and Petro, S. H. (2005). "Integral Abutments and Jointless Bridges (IAJB) 2004 Survey Summary." *Integral Abutments and Jointless Bridges 2005*, FHWA, Baltimore, MA, 12-29.

Mofarraj, B., and Zornberg, J. G. (2022). "Field Monitoring of Soil-Structure Interaction in Semi-Integral Bridges." *Geo-Congress 2022*, ASCE, Charlotte, NC, 33–42.

Ooi, P. S. K., Lin, X., and Hamada, H. S. (2010). "Field Behavior of an Integral Abutment Bridge Supported on Drilled Shafts." *J. Bridge Eng.*, 15 (1), 4–18.

Purvis, R. L., and Berger, R. H. (1983). “Bridge Joint Maintenance.” *Transportation Research Record*, 899, 1-10.

Texas Department of Transportation. (1999). *Tex-132-E: Test Procedure for Texas Cone Penetration*. Texas Department of Transportation.

Touma, F. T., and Reese, L. C. (1972). *The Behavior of Axially Loaded Drilled Shafts in Sand*. Center for Highway Research, The University of Texas at Austin.

Wang, S. T., Vasquez, L. G., Arrellaga, J. A., and Isenhower, W. M. (2020). *LPILE v2022 User’s Manual*. Ensoft Inc., Austin, TX.